

GENERALIZED EINSTEIN – ROSEN BRIDGE INSIDE BLACK HOLES

V. I. Dokuchaev^{*}, K. E. Prokopen^{**}*Institute for Nuclear Research of the Russian Academy of Sciences
117312 Moscow, Russia*Received January 19, 2024,
revised version February 9, 2024,
Accepted for publication February 10, 2024

We generalize the notion of Einstein – Rosen bridge by defining it as a space-like connection between two universes with regions of asymptotically minkowskian space-time infinities. The corresponding symmetry and asymmetry properties of the generalized Einstein – Rosen bridge are considered at the cases of Reissner – Nordström and Kerr metrics. We elucidate the versatility of intriguing symmetry and asymmetry phenomena outside and inside black holes. For description of the test particle (planet and photon) motion it is used the Kerr – Newman metric of the rotating and electrically charged black hole. It is demonstrated the symmetry and asymmetry of the one-way Einstein – Rosen bridge inside black hole space-time toward and through the plethora of endless and infinite universes.

DOI: 10.31857/S0044451024060063

1. INTRODUCTION

In this paper, we generalize the notion of Einstein – Rosen bridge by defining it as a space-like connection between two universes with regions of asymptotically minkowskian space-time infinities. The corresponding symmetry and asymmetry properties of the generalized Einstein – Rosen bridge are considered at the cases of Reissner – Nordström and Kerr metrics. We elucidate the versatility of intriguing symmetry and asymmetry phenomena outside and inside black holes. For description of the test particle (planet and photon) motion it is used the Kerr – Newman metric of the rotating and electrically charged black hole. It is demonstrated the symmetry and asymmetry of the one-way Einstein – Rosen bridge inside black hole toward and through the plethora of endless and infinite universes.

It seems that the original idea of an infinite series of bridges between universes in the Kerr metric belongs to Boyer and Lindquist [1]. The Reissner – Nordström and Kerr one-way bridge is discussed in Chapter 6.5 of Carroll’s textbook [2] and also in Chapters 3.5 and 4.4 of Ullmann’s textbook [3]. The last book also points to the physical obstacles to the existence of such a bridge between universes, which can be associated

with various types of instabilities (including quantum ones), which are discussed for example in [4,5] and more modern attempts [6]. However, the problem still remains open. Recently symmetrical geodesic motion, bound and unbound orbits and the possibility of passing through the Reissner – Nordström and Kerr bridge are also analyzed in [7] and [8] respectively.

2. BASICS OF THE KERR – NEWMAN METRIC

The famous Kerr – Newman metric or geometry (see e. g., [9–13]), which is the exact solution of Einstein’s equations [14–20] for a rotating and electrically black hole, is

$$ds^2 = -\frac{\Delta}{\Sigma}[dt - a \sin^2 \theta d\varphi]^2 + \frac{\sin^2 \theta}{\Sigma}[(r^2 + a^2)d\varphi - a dt]^2 + \frac{\Sigma}{\Delta}dr^2 + \Sigma d\theta^2, \quad (1)$$

where (r, θ, ϕ) are spherical coordinates and t is the time of static distant observer at the asymptotically radial infinity. In this metric

$$\Delta = r^2 - 2Mr + a^2 + q^2, \quad (2)$$

$$\Sigma = r^2 + a^2 \cos^2 \theta, \quad (3)$$

M — black hole mass, q — black hole electric charge, $a = J/M$ — specific black hole angular momentum (spin). The two roots of equation $\Delta = 0$ are

$$r_{\pm} = M \pm \sqrt{M^2 - a^2 - q^2}, \quad (4)$$

* E-mail: dokuchaev@inr.ac.ru

** E-mail: d1vais@yandex.ru

the event horizon of the black hole and

$$r_- = M - \sqrt{M^2 - a^2 - q^2}, \quad (5)$$

the internal Cauchy horizon of the black hole. In this paper we consider Kerr metric with the black hole event horizon, corresponding to $a^2 + q^2 \leq M$.

For simplification of equation and presentation of Figures we will often use units $G = 1, c = 1, M = 1$, and corresponding dimensionless parameters: radius $r \Rightarrow r/M$, time $t \Rightarrow t/M$, black hole spin $a \Rightarrow a/M$ and black hole charge $q \Rightarrow q/M$.

In the Kerr–Newman metric there the following integrals of motion for test particles [10]: μ — particle mass, E — particle total energy, L — particle azimuthal angular momentum and Q — the so-called Carter constant, related with the non-equatorial particle motion.

The corresponding equations of test particle motion in the Kerr–Newman metric in the differential form are [10–13]

$$\Sigma \frac{dr}{d\tau} = \sqrt{R}, \quad (6)$$

$$\Sigma \frac{d\theta}{d\tau} = \sqrt{\Theta}, \quad (7)$$

$$\Sigma \frac{d\varphi}{d\tau} = - \left(aE - \frac{L}{\sin^2 \theta} \right) + \frac{a}{\Delta} P, \quad (8)$$

$$\Sigma \frac{dt}{d\tau} = -a(aE \sin^2 \theta - L) + (r^2 + a^2) \frac{P}{\Delta}. \quad (9)$$

Here

$$P = E(r^2 + a^2) - aL + \epsilon qr, \quad (10)$$

τ — the proper time of a test massive particle or an affine parameter along the trajectory of a massless particle ($\mu = 0$) like photon, ϵ — the electric charge of test particle. Respectively, the effective radial potential $R(r)$ is

$$R(r) = P^2 - \Delta [\mu^2 r^2 + (L - aE)^2 + Q], \quad (11)$$

and the effective polar potential $\Theta(\theta)$ is

$$\Theta(\theta) = Q - \cos^2 \theta [a^2(\mu^2 - E^2) + L^2 \sin^{-2} \theta]. \quad (12)$$

Trajectories of massive particles ($\mu \neq 0$) depend on three parameters: $\gamma = E/\mu$, $\lambda = L/\mu$ and Q/μ^2 . Meantime, trajectories of massless particles like photons (the null geodesics) depend only on two parameters: λ and Q .

The nontrivial specific feature of the rotating Kerr black hole ($a \neq 0$) is the existence of so-called *ergosphere* [12, 13, 17, 19, 20] with the outer boundary

$$r_{\text{ES}}(\theta) = 1 + \sqrt{1 - q^2 - a^2 \cos^2 \theta}. \quad (13)$$

Inside the ergosphere any test object is dragged into insuperable rotation around black hole with infinite azimuthal winding by approaching the black hole event horizon. Note that the winding effect was discussed also in [8, 21].

In the following Sections we will describe the symmetry and asymmetry of test object motion in the gravitational field of the Kerr–Newman black hole. We use equations of motion in the Kerr–Newman metric (6)–(9) in our analytic and numerical calculations of test particle geodesic trajectories [22–32].

3. ONE-WAY EINSTEIN–ROSEN BRIDGE INSIDE BLACK HOLE

We start to elucidate the versatility of intriguing symmetry and asymmetry phenomena outside and inside black holes by using the Carter–Penrose diagrams (for details see, i. e., [12, 13, 17, 18]), describing in particular the global space-time structure of black holes. The evident manifestation of *symmetry* of this global structure is infinite space volumes as outside and inside the black hole event horizon. See in Fig. 1 the corresponding Carter–Penrose diagram for the Reissner–Nordström black hole, which is a special spherically *symmetric* case of Kerr–Newman black hole without rotation, i. e., $a = 0$ but $q \neq 0$. From the pure geometric point of view this diagram is both left-right and up-down symmetric. On the contrary, from the physical or space-time point view this diagram is absolutely *asymmetric* due to the inexorable upward flow of time not only at this diagram but throughout the whole universe. More precisely it means that in the General Relativity all objects are allowed to move only inside the upward directed light cones (at $\pm 45^\circ$ with respect to the upward direction. The upward directed light cone is the inexorable *asymmetry* of the world.

2D presentation of the voyage through the interiors of Reissner–Nordström black hole with interiors by using the Einstein–Rosen bridge is shown in Fig. 2. The electric charge of the black hole is $e = 0.99$. A test planet (or spaceship) with the electric charge $\epsilon = -1.5$ is periodically orbiting around black holes with orbital parameters $\gamma = 0.5$, $\lambda = 0.5$, corresponding to the maximal radius (apogee) $r_{\text{max}} = 1.65$ and minimal radius (perigee) $r_{\text{min}} = 0.29$, respectively, in dimensional units.

The periodic planet geodesic trajectories (magenta curves, both at Fig. 2 and Fig. 4), were calculated numerically by using equations of motion (6)–(9) for mas-

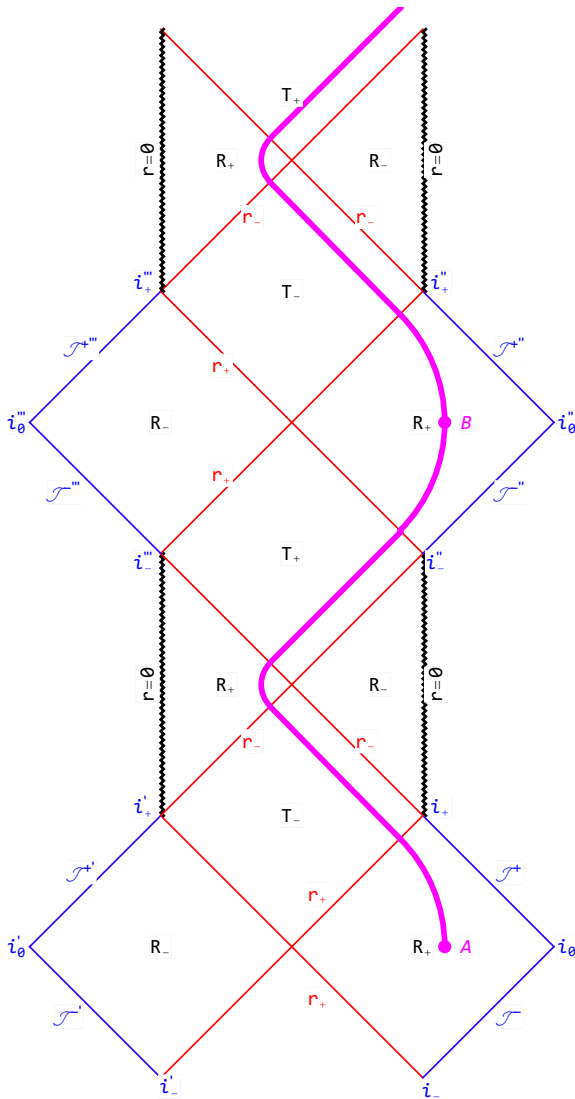


Fig. 1. Carter–Penrose diagram for the spherically symmetric Reissner–Nordström black hole with electric charge $q = 0.99$. The spaceship starts from the point A at R_+ -region toward its multi-planetary future inside the black hole. The astronauts are planning to use the Einstein–Rosen bridge (magenta curve) and intersect both the black hole event horizon r_+ and Cauchy horizon r_- at finite their proper time. After appearing near the black hole singularity at $r = 0$, the spaceship uses its powerful engines to change the direction of motion and escape the tidal destruction at small radii. In result, the voyage is happily finishing at point B (may be at the Earth-like planet) in another infinite universe. The symmetry is in possibility to repeat the complete route of this voyage starting from the point B but only in the forward direction in time toward another multi-planetary future. It is impossible to return the native Earth due to impossibility of any motion beyond the light cone. This is the motion *asymmetry* on the one-way Einstein–Rosen bridge inside black hole

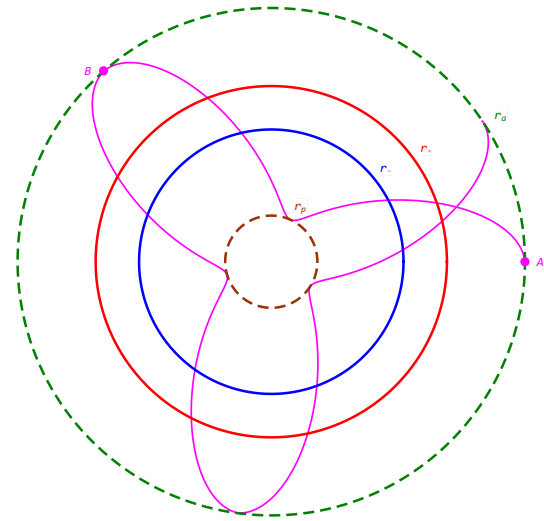


Fig. 2. 2D presentation of the voyage through the Reissner–Nordström black hole interiors by using the Einstein–Rosen bridge. This picture is geometrically absolutely *symmetric* or, in other words, it is nicely *symmetric*. At the same time, this picture is misleading and physically controversial: Indeed, the voyage is starting at apogee r_a from the position at point A , then reach the perigee r_p and return the apogee r_a at the point B for a finite proper time, demonstrating the absolute geometric *symmetry*. Meanwhile, there is a crucial hitch: this apogee r_a at the point B is not in the native universe, but in the other quite distant universe, as it is clearly viewed at the Carter–Penrose diagram in Fig. 1. The apogee r_a and perigee r_p radii are shown by dashed circles. Respectively, the event radii of event horizon r_+ and Cauchy horizon r_- are shown by solid circles. The magenta curve here and in the Fig. 4 is numerically calculated geodesic trajectory with using equations of motion (6)–(9) for massive test particles ($\mu \neq 0$)

sive test particles ($\mu \neq 0$). Note, that the periodical motion of the test planet is limited in time due to energy losses in inevitable emission of the gravitational waves.

The picture in Fig. 2 is geometrically absolutely *symmetric* or, in other words, it is completely or nicely *symmetric*. The geodesic trajectories of test planet ($\mu \neq 0$) in this Fig. 2 and in Fig. 3 (the red curves), are numerically calculated [22–32], by using the corresponding equations of motion in the Kerr–Newman metric (6)–(9).

At the same time, this picture is misleading and physically controversial: Indeed, the voyage is starting at apogee r_a from the position at point A , then reach the perigee r_p and return the apogee r_a at the point B for a finite proper time, demonstrating the abso-

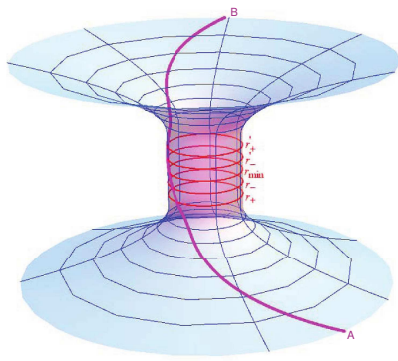


Fig. 3. Embedding diagram for the voyage through black hole interiors by using the Einstein–Rosen bridge. This bridge connects two asymptotically flat universes like wormhole tunnel, but with the only one-way motion from the initial point *A* to the final point *B*. The geometrical *symmetry* of this embedding diagram is deceptive. In fact, this embedding diagram demonstrate the *asymmetric* space-time origin of the one-way Einstein–Rosen bridge (remember about loss-cone)

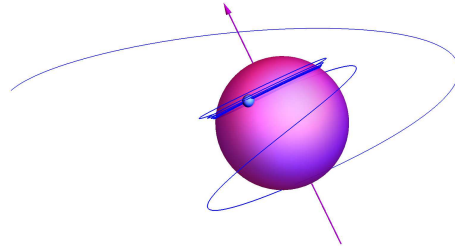


Fig. 5. Trajectory of the test planet ($\mu \neq 0$) with orbital parameters $\gamma = 0.85$, $\lambda = 1.7$ and $Q = 1$ plunging into the fast-rotating Kerr black hole with spin $a = 0.9982$. This test planet starts from the *upper* hemisphere very far from the black hole. Inside the ergosphere (13) this planet is winding up on the black hole event horizon *higher* the black hole equatorial plane. Blue curve here is the numerically calculated geodesic trajectory with using equations of motion (6)–(9) for test particles

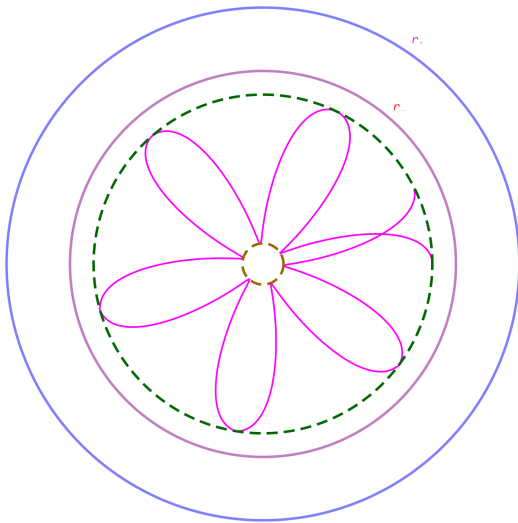


Fig. 4. Both the geometrical and physical completely *symmetric* picture of the periodic orbital motion of the test planet or spaceship around the central singularity of the Reissner–Nordström black hole inside the Cauchy horizon r_- . The *asymmetric* Reissner–Nordström bridge is only needed for penetration into this very exotic region at $0 < r < r_-$, where exist the nearly stable periodic orbits for test particles, which are very similar to the periodic orbits outside the black hole event horizon r_+ . The apogee r_a and perigee r_p radii are shown by dashed circles. Respectively, the event radii of event horizon r_+ and Cauchy horizon r_- are shown by solid circles

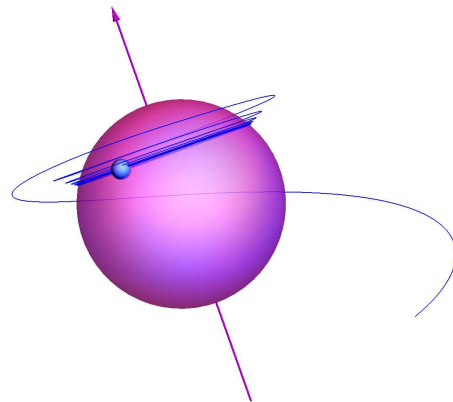


Fig. 6. Trajectory of the test planet ($\mu \neq 0$) with orbital parameters $\gamma = 0.85$, $\lambda = 1.7$ and $Q = 1$ plunging into the fast-rotating Kerr black hole with spin $a = 0.9982$. This test planet starts from the *lower* hemisphere very far from the black hole. Inside the ergosphere this planet is winding up on the black hole event horizon *higher* the black hole equatorial plane. Blue curve here is the numerically calculated geodesic trajectory with using equations of motion (6)–(9) for test particles

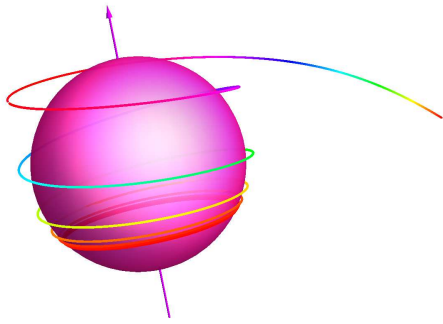


Fig. 7. Photon trajectory with orbital parameters $\lambda = 2$ and $Q = 1$. This photon is plunging into the fast-rotating Kerr black hole with $a = 0.9982$ and is winding up on the black hole event horizon below the equatorial plane. Multi-colored curve is the numerically calculated geodesic trajectory with using equations of motion (6)–(9) for massless test particles like

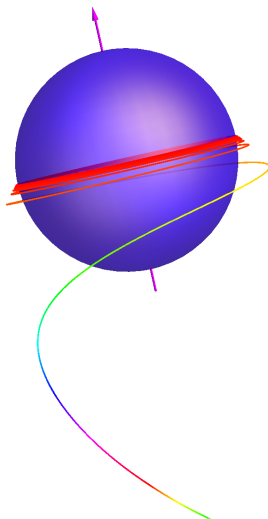


Fig. 8. Numerically calculated photon ($\mu = 0$) trajectory with orbital parameters $\lambda = -1.493$ and $Q = 12.99$, which is plunging into the fast-rotating Kerr black hole with spin $a = 0.9982$. It must be stressed that at large distances from black hole the test particle with negative azimuthal angular momentum ($\lambda = -2.811$) rotates in opposite direction with respect to the black hole. Meanwhile, by approaching the black hole (*inside the ergosphere*) test particle is forced to rotate in the same direction as black hole

lute geometric *symmetry*. Meanwhile, there is a crucial hitch: this apogee r_a at the point B is not in the native universe, but in the other quite distant universe, as it is clearly viewed at the Carter–Penrose diagram in Fig. 1. This hitch again destroys the Einstein–Rosen bridge *symmetry*.

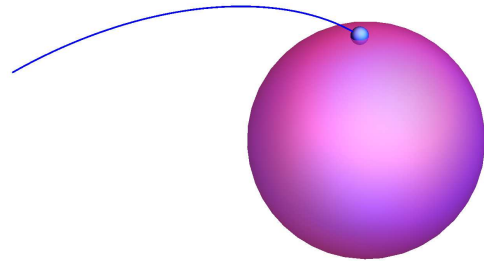


Fig. 9. A trivial but though very expressive trajectory of a test planet ($\mu \neq 0$) with parameters $\gamma = 1$, $\lambda = 1$ and $Q = 0.5$, which is plunging into the spherically *symmetric* and nonrotating Schwarzschild black hole (with both the spin $a = 0$ and electric charge $q = 0$). The starting point for this numerically calculated crazy voyage is at the radial distance $r = 6$

Figure 3 shows the embedding diagram for the voyage through black hole interiors by using the Einstein–Rosen bridge. The embedding diagram is very useful for the training of intuitive understanding of the peculiarities of the enigmatic black holes. In this embedding diagram the Einstein–Rosen bridge connects two asymptotically flat universes like wormhole tunnel [33, 34], but with the only one-way motion from the initial point A to the final point B . The geometrical *symmetry* of this embedding diagram is deceptive. In fact, this embedding diagram demonstrate the *asymmetric* space-time origin of the one-way Einstein–Rosen bridge (remember about loss-cone).

The completely *symmetric* picture of the periodic orbital motion of the test planet or spaceship around the central singularity of the Reissner–Nordström black hole inside the Cauchy horizon r_- is shown in Fig. 4. The electric charge of the black hole is $e = 0.99$ and test planet (or spaceship) with the electric charge $\varepsilon = -1.5$ is periodically orbiting around black holes with orbital parameters $\gamma = 1.7$, $\lambda = 0.1$, corresponding to the maximal radius (apogee) $r_{\max} = 0.75$ and minimal radius (perigee) $r_{\min} = 0.09$, respectively. The *asymmetric* Reissner–Nordström bridge is only needed for penetration into this very exotic region at $0 < r < r_-$, where exist the nearly stable periodic orbits for test particles [35–41], which are very similar to the periodic orbits outside the black hole event horizon r_+ .

4. SYMMETRY AND ASYMMETRY OF TEST PARTICLE TRAJECTORIES NEAR ROTATING BLACK HOLE

Figures 5–7 demonstrate both *symmetry* and *asymmetry* features of massive and massless particle trajectories plunging into rotating Kerr black hole with spin $a = 0.9982$. Magenta arrows shows the direction of the black hole rotation in accordance with the gimlet rule. The multi-colored curves at Figs. 7 and 8 are the geodesic trajectories for massless test particles like photons ($\mu = 0$) numerically calculated with using equations of motion (6)–(9). By approaching the black hole, the trajectories of all particles, both massive and massless ones, are infinitely winding up on the black hole event horizon in the direction of the black hole rotation and at the fixed latitudes. This winding up is a manifestation of *symmetry* of behavior of all trajectories, plunging into rotating black hole. At the same the direction of the black hole rotation is a corresponding manifestation of *asymmetry* of the gravitational field of the Kerr metric.

At last, for completeness of black hole *symmetric* and *asymmetric* properties, at Fig. 9 is shown the trajectory of the test planet ($\mu \neq 0$) with parameters $\gamma = 1$, $\lambda = 1$ and $Q = 0.5$. This test planet is plunging into the spherically *symmetric* and nonrotating Schwarzschild black hole (with both the spin $a = 0$ and electric charge $q = 0$), starting from the radial distance $r = 6$. It must be especially checked that the traversable (though only one-way in time and direction) Einstein–Rosen bridge is absent at all inside the Schwarzschild black hole (see for details, e. g., [12, 14]).

5. CONCLUSION AND DISCUSSION

It is demonstrated the symmetry and asymmetry of the voyage on one-way Einstein–Rosen bridge inside black hole toward the endless multiplanetary future. The apparent symmetry of both the Carter–Penrose and embedding diagrams is mainly related with a pure geometrical vision of this phenomenon. Quite the contrary, the physical (space-time) vision elucidates the absolute asymmetry of the Einstein–Rosen bridge due to existence of the light-cone limitation for possible motions.

Note, that the traversable (though only one-way in time and direction) Einstein–Rosen bridge exist only in the case of both rotating Kerr $a \neq 0$ and electrically charged Reissner–Nordström $q \neq 0$ black holes. It is absent at all inside the Schwarzschild black hole (see for details, e. g., [12, 14])

The infinite winding up of trajectories of all particles on the black hole event horizon is a manifestation of *symmetry* behavior of all trajectories, plunging into rotating black hole. At the same time, the fixed direction in space of the black hole rotation axis is a strict manifestation of the Kerr metric both *symmetry* and *asymmetry*.

Acknowledgments. We are grateful to E. O. Babichev, V. A. Berezin, Yu. N. Eroshenko, N. O. Nazarova and A. L. Smirnov for stimulating discussions. Authors also are very indebted to anonymous reviewer for suitable references and historical remarks which improve the presentation of paper.

REFERENCES

1. R. H. Boyer and R. W. Lindquist, J. Math. Phys. **8**, 265 (1967).
2. S. Carroll, *An Introduction to General Relativity, new international edition*, Pearson (2014), p. 257.
3. V. Ullmann, *Gravity, Black Holes and the Physics of Time-Space*; Czechoslovak Astronomic Society, CSAV, Ostrava, (Online version in English: <https://astronuclphysics.info/GravitCerneDiry.htm>) (1986).
4. Y. Giiresel, V. D. Sandberg, I. D. Novikov, and A.A. Starobinskij, Phys. Rev. D **19**, 413 (1979).
5. M. Simpson and R. Penrose, Int. J. Theor. Phys. **7**, 183 (1973).
6. R. DeMott, S. DeMott, and A. DeMott, Class. Quant. Grav. **39**, 195015 (2022).
7. D. Abramson, Thai J. of Phys. **38**, 69 (2021).
8. C. Dyson and M. van de Meent, Class. Quant. Grav. **40**, 195026 (2023).
9. R. P. Kerr, Phys. Rev. Lett. **11**, 237 (1963).
10. B. Carter, Phys. Rev. **174**, 1559 (1968).
11. I. D. Novikov, and K. S. Thorne, in *Black Holes*, ed. by C. DeWitt and B. S. DeWitt, Gordon and Breach, New York (1973), p. 343.
12. C. W. Misner, K. S. Thorne, and J. A. Wheeler, *Gravitation*, W. H. Freeman, San Francisco, CA, USA (1973).
13. S. Chandrasekhar, *The Mathematical Theory of Black Holes*, in *The International Series of Monograph on Physics*, Clarendon Press, Oxford (1983), Vol. 69, Chap. 7.

14. R. Penrose, *Structure of Space-Time. Battelle Rencontres 1967. Lectures in Mathematical Physics*, Chap. VII, ed. by C. M. Dewitt and J. A. Wheeler, W. A. Benjamin, Inc., New York–Amsterdam (1968), Chap. 2.
15. J. M. Bardeen, in *Black Holes*, ed. by C. DeWitt and B. S. DeWitt, Gordon and Breach Science Publishers, New York (1973), p. 215.
16. Y. Choquet-Bruhat, C. DeWitt-Morette, and M. Dillard-Bleick, *Analysis, Manifolds and Physics, Part 1, Basics*, Elsevier Science, Amsterdam (1977), Chap. V.
17. R. M. Wald, *General Relativity*, The Univ. of Chicago Press, Chicago (1984).
18. S. W. Hawking, and G. F. R. Ellis, *The Large-Scale Structure of Space-Time*, Cambridge Monographs on Mathematical Physics, Cambridge University Press, Cambridge (2011).
19. J. M. Bardeen, W. H. Press, and S. A. Teukolsky, *Rotating Black Holes: Locally Nonrotating Frames, Energy Extraction, and Scalar Synchrotron Radiation*, *Astrophys. J.* **178**, 347 (1972).
20. J. M. Bardeen, B. Carter, and S. W. Hawking, *Commun. Math. Phys.* **31**, 161 (1973).
21. T. P. Kling, E. Grotzke, K. Roebuck, and H. Roebuck, *Gen. Rel. Grav.* **51**, 32 (2019).
22. E. O. Babichev, V. I. Dokuchaev, and Yu. N. Eroshenko, *Uspekhi Fiz. Nauk* **183** 1257 (2013) [*Phys. Usp.* **56**, 1155 (2013)].
23. V. I. Dokuchaev, *GRG* **46**, 1832 (2014).
24. V. I. Dokuchaev and Yu. N. Eroshenko, *Uspekhi Fiz. Nauk* **185** 829 (2015) [*Phys. Usp.* **58**, 772 (2015)].
25. V. I. Dokuchaev and Yu. N. Eroshenko, *Pisma JETP* **101**, 875 (2015) [*JETP Lett.* **101**, 777 (2015)].
26. V. I. Dokuchaev and N. O. Nazarova, *J. High Energy Phys. Lett.* **106**, 637 (2017).
27. V. I. Dokuchaev and N. O. Nazarova, <https://youtu.be/P6DneV0vk7U> (2017).
28. V. I. Dokuchaev and N. O. Nazarova, *ZhETF* **155**, 677 (2019) [*JETP* **128**, 578 (2019)].
29. V. I. Dokuchaev, N. O. Nazarova, and V. P. Smirnov, *GRG* **51**, 81 (2019).
30. V. I. Dokuchaev, and N. O. Nazarova, *Universe* **5**, 183 (2019).
31. V. I. Dokuchaev, *IJMPD* **28**, 1941005 (2019).
32. V. I. Dokuchaev, and N. O. Nazarova, <https://youtu.be/fps-3frL0AM> (2019).
33. J. A. Wheeler, *Geometrodynamics*, Academic Press, New York (1962).
34. M. S. Morris and K. S. Thorne, *Am. J. Phys.* **56**, 395 (1988).
35. J. Bičák, Z. Stuchlík, and V. Balek, *Bull. Astron. Inst. Czech.* **40**, 65 (1989).
36. V. Balek, J. Bičák, and Z. Stuchlík, *Bull. Astron. Inst. Czech.* **40**, 133 (1989).
37. S. Grunau and S. Kagramanova, *Phys. Rev. D* **83**, 044009 (2011).
38. M. Olivares, J. Saavedra, C. Leiva, and J. R. Vilanueva, *Mod. Phys. Lett. A* **26**, 2923 (2011).
39. E. Hackmann, V. Kagramanova, J. Kunz, and C. Lamünerzahl, *Phys. Rev. D* **81**, 044020 (2010).
40. D. Pugliese, H. Quevedo, and R. Ruffini, *Phys. Rev. D* **83**, 024021, 23pp. (2011).
41. V. I. Dokuchaev, *CQG* **28**, 235015 (2008).